Evaluation of Fish-Injury Mechanisms During Exposure to a High-Velocity Jet

United States
Department of Energy

Evaluation of Fish-Injury Mechanisms
During Exposure to a High-Velocity Jet

Gregory R. Guensch
Robert P. Mueller
Craig A. McKinstry
Dennis D. Dauble
Pacific Northwest National Laboratory

November 2002

DISCLAIMER

This report was prepared as an account of work sponsored by an agency of the United States Government. Neither the United States Government nor any agency thereof, nor Battelle Memorial Institute, nor any of their employees, makes any warranty, express or implied, or assumes any legal liability or responsibility for the accuracy, completeness, or usefulness of any information, apparatus, product, or process disclosed, or represents that its use would not infringe privately owned rights. Reference herein to any specific commercial product, process, or service by trade name, trademark, manufacturer, or otherwise does not necessarily constitute or imply its endorsement, recommendation, or favoring by the United States Government or any agency thereof, or Battelle Memorial Institute. The views and opinions of authors expressed herein do not necessarily state or reflect those of the United States Government or any agency thereof.

<div align="center">

PACIFIC NORTHWEST NATIONAL LABORATORY
operated by
BATTELLE
for the
UNITED STATES DEPARTMENT OF ENERGY
under Contract DE-AC06-76RL01830

PNNL-14173

</div>

Summary

As part of the research supported by U.S. Department of Energy (DOE) Advanced Hydropower Turbine System (AHTS) Program, the Pacific Northwest National Laboratory (PNNL) conducted a study where age-0 and age-1 chinook salmon, as well as several other types of fish, were released into a submerged water jet to quantify injuries caused by shear stresses and turbulence (Neitzel et al. 2000). The fish releases were videotaped. These videotape records were digitized and analyzed using new methods to identify the injury mechanisms and the stresses involved.

Visible external injuries sustained by fish in this study generally occurred during the initial contact with the jet and not during the tumbling that occurred after the fish fully entered the turbulent flow. The inertial stresses of tumbling, however, may cause temporary or even permanent vestibular and neurological injuries. Such injuries can result in disorientation and loss of equilibrium, which are life threatening in the "natural" environment.

Operculum injuries predominated at moderate water jet speeds (12 and 15 m·s^{-1}). At the highest speed, eye, operculum, isthmus, and gill injuries were equally common, and disorientation was most common. Bruising and descaling were relatively rare, especially for age-0 fish.

Age-0 fish were less susceptible than the larger age-1 fish to all visible injury types, especially at lower speeds. This is presumably because age-0 fish have less mass and inertia, and therefore sustain smaller forces on exposed organs during acceleration. Alternatively, age-0 fish were substantially more susceptible to behavioral impairments such as disorientation. This may also relate to the smaller mass of the age-0 fish. The less massive age-0 fish sustain larger accelerations and jerks, which may be important sources of the internal injuries to the vestibular and neurological systems.

All the dynamic parameters computed from the bulk motion of the fish (velocity, jerk, and force) were positively correlated with injury level, based on the results of this study. Multinomial response model results further suggested that force is most predictive of injury.

Acknowledgments

Contents

Figures

Tables

Glossary

AHTS   Advanced Hydropower Turbine System Program

DOE   U.S. Department of Energy

FL   fork length

fps   feet per second

PIV   Particle Image Velocimetry

PNNL   Pacific Northwest National Laboratory

VFM   virtual fish model

1.0   Introduction

As part of the research program supported by U.S. Department of Energy Advanced Hydropower Turbine System (AHTS) Program, Pacific Northwest National Laboratory (PNNL) staff conducted a study where fish were released into a submerged water jet of known characteristics to quantify the injurious shear stresses and turbulence levels (Neitzel et al. 2000). The fish releases were videotaped to allow detailed observation of the release and injury mechanisms. These video records have been analyzed using new methods to identify the mechanisms of injury and the stresses involved. The video records revealed the general pattern of a fish release in the 2000 study as well as details such as the point at which one or both opercula flare forward or eye damage occurs. The videos also showed that fish generally turn to one side or the other after contacting the water jet, and that bending and twisting occurs once fish enter the jet flow. Further, specific types of injuries and the events leading to them were shown. The interpretation of the results from the Neitzel et al. (2000) study have been refined in this report using these insights.

The videos also provide information to support a more quantitative analysis of the dynamic parameters involved. The displacement, orientation, and deformation can be determined using the fish positions and the time stamp on each video frame. From this information, additional parameters such as velocity, acceleration, impulse, force, and jerk can be calculated that quantify the stresses to which the fish are subjected. The analysis of these parameters, summarized in this report, emphasizes the information relevant to future biomechanical testing of fish injury thresholds and tissue properties, and the eventual development of a virtual (computational) fish model (VFM) that will allow assessment of fish injury potential in simulated flow fields. To create the VFM, results from direct biomechanical tests and precisely controlled fish tests hydraulic environment using Particle Image Velocimetry (PIV) equipment will be used to assign physical properties and injury criteria to our detailed morphometric fish model generated from a Nuclear Magnetic Resonance scan of a real fish. The VFM can then be incorporated into a geometry-based computational fluid-structure interaction model that can simulate the complex hydraulic conditions in hydropower systems and their effect on fish.

The primary objective of this video analysis is to determine whether type of injury or injury level as a whole correlate to variables that can be measured or estimated from the fish-release video records. Injury level is determined subjectively for each fish from severity and number of injuries as described in the methods. Peak and average values of the following variables are considered:

- Fish velocity (v)
- Acceleration (a)
- Impulse (I)
- Force (F)
- Jerk (J, rate of change of acceleration).

Acceleration is of interest because it is an indicator of the impulse and force on the fish, which should be the source of many injuries. The potential for the force on the fish to cause injury is especially high in these test releases because as the slow moving fish comes in contact with the high velocity jet, the bulk of the force is generally applied to only a small area such as the gill or eye. Jerk is used commonly in automotive engineering when evaluating severity in impact tests. It is related to injury potential because when the acceleration of a complex body is unsteady, different body parts respond differently. For example, in a suddenly stopping car, the head is thrown forward. In PNNL's tests, an analogous situation occurred where during a fish release the opercula are flared forward and torn as the mass of the body is left behind.

2.0   Methods

2.1   Test Fish

Neitzel et al. (2000) used rainbow trout and steelhead (*Oncorhynchus mykiss*), spring and fall chinook salmon (*O. tshawytscha*), and American shad (*Alosa sapidissima*) in their tests. Rainbow trout were raised at the aquatic laboratory at PNNL. Steelhead (Skamainia strain) were from Beaver Creek Hatchery, Washington. Spring chinook salmon were from Leavenworth National Fish Hatchery, Washington, and fall chinook salmon were from Priest Rapids Hatchery, Washington. American shad were collected from the McNary Dam juvenile passage facility at Columbia River km 469. Fish ranged from 8.5 to 21 cm in length, had minimal scale loss, and were representative of anadromous fish populations migrating downstream past hydroelectric dams. With the exception of hatchery-reared rainbow trout, test fish were in the smoltification life stage or were active migrants.

The video analysis concentrates primarily on the chinook salmon because that group offered the largest sample size of comparable fish. Two life stages of fall chinook were tested: subyearling (age 0) and yearling (age 1). The fork length (FL) ranged from 81 to 95 mm (mean 85) for the subyearling chinook and from 123 to 150 mm (mean 138) for the age-1 fish. Spring chinook salmon ranged from 135 to 157 mm FL (mean 145). Average fish masses were 5.5 g for age-0 fish and 33.7 g for age-1 fish.

2.2   Test System

A rectangular flume (Figure 1) containing a submerged water jet was used to create a quantifiable shear environment consistent with conditions expected within a hydroelectric turbine. The flume was 9 m long by 1.2 m wide by 1.2 m deep when filled with water. A conical stainless-steel nozzle that began at 25.4 cm diameter and constricted to a circular 6.35 cm diameter over 50.8 cm in length was bolted to a flange inside the flume (Figure 2). This nozzle configuration provided a contraction ratio of 5:1 that effectively accelerated flow and reduced non-uniformity in the inlet velocity distribution. The

Figure 1. Test flume shown in foreground.
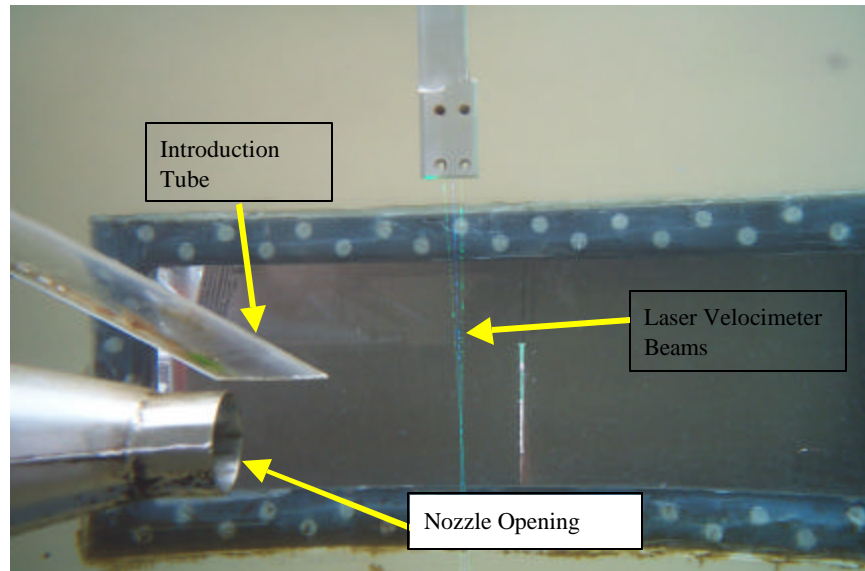
Figure 2. Test system, including nozzle opening, introduction tube, laser velocimeter beams, and one of the side viewing windows.

pump/nozzle system was capable of creating exit velocities in excess of 20 m·s^{-1}. Viewing windows are located on the side and bottom at the nozzle end of the flume to record fish reactions as they enter test flow fields.

The nozzle exit was submerged under about 0.6 m of water during all tests. Fish were introduced immediately above the jet and in front of the nozzle through a Plexiglas® deployment tube fastened above the nozzle at an angle of 30° (Figure 2). The terminus of the deployment tube was just above the terminus of the nozzle, with a 1-cm horizontal separation. This small separation width prevented any fish from exiting the test without being subjected to the shear environment.

Fish were exposed to the following water jet velocities: 3, 6, 9, 12, 15, and 18 m·s^{-1} (10, 20, 30, 40, 50, and 60 feet per second (fps)). The flow field was characterized using a Pitot tube and a laser velocimeter. From this information, relationships between fish injury and fluid strain rate, shear stress, and turbulence were investigated. See Neitzel et al. (2000) for more information on the study.

Video images of exposed fish were captured using two identical high-speed cameras (Redlake Imaging MotionScope^{TM} 1000S) positioned to view fish as they exited the tube. The cameras captured a side (X-Y) and bottom view (Y-Z or X-Z plane). The video cameras were situated near the viewing panels and connected to processors located in a nearby office trailer. The cameras recorded fish orientation and location from the moment a fish descended the introduction tube and contacted the shear environment, until it was swept out of the immediate shear environment (~0.5 m [1.6 ft]). An entire exposure sequence lasted only a fraction of a second. Cameras recorded each event simultaneously at 500 frames per second, which provided an approximate 2-s buffer of stored memory. A tape reviewer recorded each event to videotape at two speeds (10 and

30 frames per second) so that specific injuries could be verified. The field of view for each system was approximately 44.4 cm (17.5 in.) vertical by 45 cm (17.7 in.) horizontal for most tests. A calibration tape was placed along the axis of the nozzle and recorded with both cameras at the beginning of each test day. The calibration data were used to determine fish position and acceleration. All recordings were made on a Sony model EVC 200 Hi 8mm tape recorder attached to a Robot model MV50 four-channel multiplexer. A video overlay board was used to record the test fish and exit velocity for each test series.

2.3 Handling of Fish

A holding/acclimation trough was installed near the test facility. Test stocks were maintained at low densities and with a high water turnover rate to maintain optimal water quality conditions during holding and acclimation periods. Test fish were loaded into the exposure system without removing them from water. They were randomly captured from the holding trough using a small section of clear tubing (cartridge) containing a small volume of water. Each fish was then transferred to the deployment tube where it would swim down the tube and exit into the flow field of the nozzle (headfirst deployment). The fish readily passed down the introduction tube and into the flow field within a few seconds. The same procedure was used for the tail first test series. Freeze branding with liquid nitrogen was used to differentiate control and test fish in the predation tests.

Once a fish was loaded into the cartridge, the pump was activated and allowed to reach the required test velocity condition. During this time (~5 s), the fish was resting in the cartridge. The exposure began when the fish was allowed to swim from the cartridge into the deployment tube and into the shear environment. The velocity used in the test was randomly selected from the following: 3, 6, 9, 12, 15, and 18 m·s^{-1} (10, 20, 30, 40, 50, and 60 fps).

After each individual exposure, the system was shut down (to avoid potential injury from multiple exposures to the shear environment), and the fish were recovered from the flume with dip nets. Recovery was also aided by the use of a brail or crowding fence to capture the fish. The fish was then placed back in the clear cartridge, and its external condition was evaluated for injuries.

For every series of tests, a control group comprising 10 fish were introduced into the deployment tube, allowed to swim out, and then recaptured with dip nets with no exposure to the shear environment (pump off). This group was used as reference for monitoring injuries of exposed fish.

After examination, each test group (including control fish) was placed in small net pens in a concrete raceway adjacent to the flume. The raceway was supplied with well water maintained at the test temperature. Test fish were held for 48 h to monitor delayed mortality or other effects indicative of stress or injury.

2.4 Characterization of Direct Injury and Mortality

Following exposure, the type and extent of the injuries sustained and the direct mortality (initial and delayed) were assessed. Evaluation of external injuries was the primary method for monitoring tissue damage and direct mortality. After initial examination, each test group (including control fish) was held for 48 h to monitor delayed mortality or other effects indicative of stress or injury (dark discoloration, lethargy, loss of equilibrium, fungal/disease infection, and osmoregulation problems).

The occurrence and severity of injuries (biological responses) were examined for each fish following the test release and recovery from the test tank. Injuries included eye damage, descaling, gill/operculum damage, isthmus damage, split fins, bruising/discoloration, and spinal fracture. Disorientation, characterized by little or no swimming ability, was also considered an indicator of potentially severe injury and impairment. In the study by Neitzel et al. (2000), minor injuries were defined as those that were visible, but not life threatening, and that disappeared within the 48 h post-exposure observation period (e.g., small bruises = 0.5 cm in diameter). In contrast, injuries that resulted in prolonged loss of equilibrium, seemed life threatening, or persisted throughout the post-exposure observation were rated as major. Examples of major injuries included large bruises (= 0.5 cm in diameter), damage to the spinal column, cuts with visible bleeding, injured eyeballs (bulged, hemorrhaged, or missing), and gill damage (inverted gill arches, or tears at the insertions of the gill arches severe enough to result in bleeding).

Injury levels were reassigned for this video analysis based on information in the injury data sheets because the injury levels were decoupled from the fish release numbers in the Neitzel et al. study. The injury levels were reassigned according to the following criteria:

- **No Injury:** No observable physical injury indicated on the data sheets or brief minor disorientation.
- **Minor Injury:** Visible but not life threatening, such as minor bruising, operculum damage, gill bleeding, isthmus tear, and/or descaling.
- **Major Injury:** Life-threatening injuries such as severe bruising, bleeding, tearing, creasing, multiple injuries, prolonged (1-2 h) swimming impairment, or disorientation.
- **Death:** Immediate or delayed mortality as a result of injuries sustained.

These injury level and injury type data were recorded for each fish released and compiled into a table to which the dynamic parameters of velocity, acceleration, jerk, impulse, and force would be added (see Appendix).

2.5 Digitizing the Releases

An imaging software program (Optimas^{TM}) was used to digitize the images. The protocol involved advancing the tape at a specific interval (two frames or 0.004 s), saving the image to file, scaling the image, setting the coordinate system, and digitizing the position

of the eye. A two-dimensional coordinate system was used where *x* was the downstream
direction and *y* was the vertical direction. The program automatically recorded a distance
measurement from the starting point, and an *x*, *y* location at each measurement. The eye
was used because no other mark was available that could be accurately tracked. The path
of the eye is considered representative of the bulk motion of the fish only for the initial
part of the release. A more sophisticated, multi-point tracking procedure is necessary
after the fish enters the jet turbulence completely and begins to exhibit multi-axis
rotational motion as shown in Figure 3. Lateral movement was minimal, especially in the
initial part of the release, and was subsequently ignored.
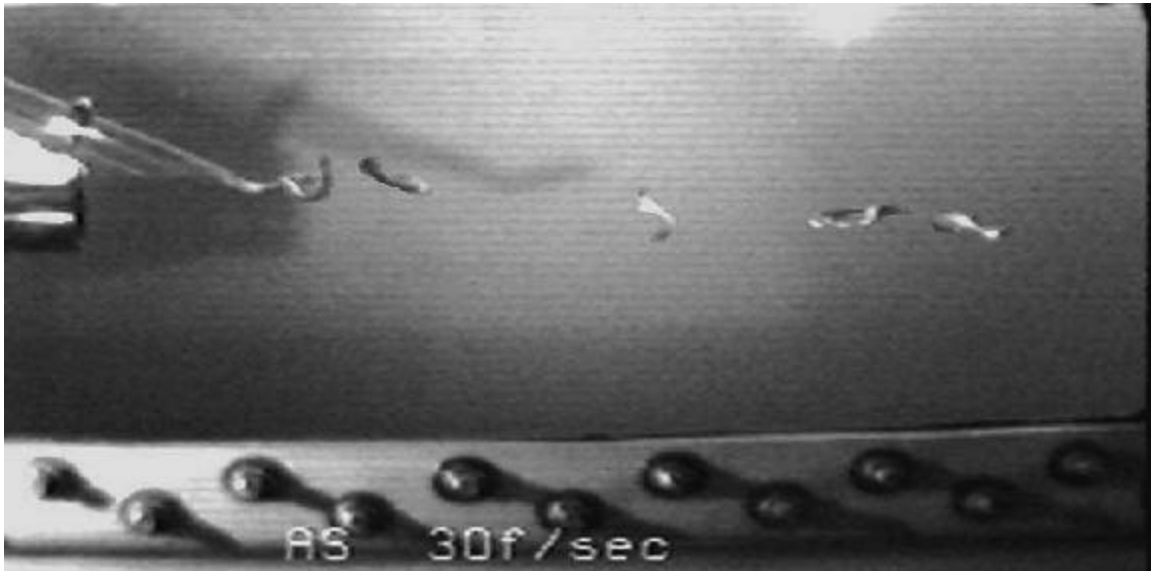
Figure 3. Combined sequence of images showing the pattern of a typical fish release.

2.6   Data Analysis

2.6.1   Computation of Dynamic Parameters

The dynamic parameter values for velocity (*v*), acceleration (*a*), jerk (*J*), impulse (*I*), and
force (*F*) were computed for the initial 0.016, 0.024, and 0.10 s of the video records
following release of 23 age-0 and 83 age-1 juvenile chinook salmon into water-jets at 40,
50, and 60 fps jet velocities. The peak value and root mean average (average of the
absolute values) were computed for each variable for each fish release. The peak value
was intended to represent the highest magnitude or most severe level of that parameter
experienced by a given fish. The root mean average was intended to summarize the
average magnitude of the level of that parameter experienced by the fish for the full time
period analyzed (e.g., 0-0.016, 0-0.024, or 0-0.1 s). These data were then summarized
and combined with the fish injury level data. See Appendix.

The dynamic parameters were computed from the change in position of the fish eye between each successive time step. Simplified expressions for each variable are shown below:

$$v = \frac{\left(dx^2 + dy^2\right)^{(1/2)}}{dt}$$

$$a = \frac{dv}{dt}$$

$$I = m \cdot dv$$

$$F = m \cdot a = \frac{I}{dt}$$

where m is the fish mass, dt is the time step (equal to the time between digitized frames, 0.004s), and changes in variables between successive digitized frames are indicated by the differential (d). For example, $dx = x_i - x_{i-1}$, where i indicates the frame number.

Given an assumed maximum error of 1 mm in each direction when digitizing points, the magnitude of potential distance error in position measurements is approximately $?_{xy} = (dx^2 + dy^2)^{1/2} = 1.4$ mm $= 0.0014$ m for a single measurement. The maximum potential error in a pair of measurements is then $2?_{xy}$. The measurement error was propagated as shown in Table 1 to approximate the error of point estimates for each parameter. Note the dramatic increase in error that occurs with successive derivatives of velocity. A small error in distance can cause a large error in jerk.

Table 1. Error estimates for each parameter.

	Formula	Age 0	Age 1
v (m s^{-1})	$2?_{xy}/dt$	0.7	0.7
a (m s^{-2})	$2?_{xy}/dt^2$	175	175
J (m s^{-3})	$2?_{xy}/dt^3$	43,750	43,750
I (kg m s^{-1})	$m \cdot 2?_{xy}/dt$	0.0039	0.24
F (kg m s^{-2})	$m \cdot 2?_{xy}/dt^2$	0.96	5.9

Overall mean masses were estimated for age-0 and age-1 fish and used to compute impulse and force for each of the fish released. Subsequently, variation in impulse and force resulting from differences in individual mass within an age class could not be resolved. In addition, because the time step (dt) was fixed, acceleration, impulse, and force are equivalent within an age class. Therefore, only velocity (v), jerk (J), and force (F) will be fully evaluated.

2.6.2 Descriptive Analysis

The following analysis was conducted to evaluate whether any of the parameters correlated with fish injury level.

1. The fish were grouped by degree of injury (i.e., no injury, minor injury, major injury or death). The dead fish were included with the major injury group because there were too few to analyze separately.

2. The average and standard deviation were computed for the **peak** value of each variable of interest. These parameters were calculated for 0.016, 0.024, and 0.10 s of the release; however, only 0.024 s results are used because video observations indicated that the visible injuries occurred at or before this time (initial contact with the jet), where the hydraulic conditions were most severe. Because an average of averages was computed for each injury level, the variance was divided by 6, which represented the subsample sizes (# of digitized points included in the average for each fish release). The standard deviation was then the square root of the variance as usual. Use of this statistic assumed applicability of the central limit theorem (Zar 1999).

3. The mean values for each injury group were plotted with error bars of one standard deviation to determine if there was any significant difference for any of the variables. The median values were plotted as comparison indices uninfluenced by outlier data values. Comparing the median and mean also provided information about the skew in the data.

2.6.3 Inferential Analysis: Multinomial Response Model

The average masses of the age-0 and age-1 groups were substantially different (5.5 g for age-0 fish and 33.7 g for age-1 fish). Subsequently, all the variables of interest (velocity, jerk, and force) were also quite different, with velocity and jerk being higher for age-0 fish and force being higher for age-1. Therefore, these groups were considered distinct populations and evaluated separately. This allowed the effect of all the variables to be evaluated without being overpowered by the obvious strong effect of fish mass. The multinomial response model was only applied to the age-1 fish because there was an insufficient number of age-0 fish (23).

As in the descriptive analysis, the peak values for each dynamic parameter were used in the inferential analysis; in contrast, the inferential analysis was also applied to parameters derived from each of the time durations (0.016, 0.024, and 0.10 s) following fish release. Correlations between the computed dynamic parameters were shown by plotting the parameters against one another.

A multinomial response model was fit separately to data derived from each of the three time-durations of video footage: 0.016-, 0.024-, and 0.10-s post-release. The response variable for each model was a three level ordered factor: 1=no injury, 2=minor injury,

3=severe injury or death. Each of the three dynamic parameter values was used individually to fit a univariate model and then ranked in descending order by the value of the likelihood ratio Chi-square statistic. Larger values in the likelihood ratio Chi-square statistic indicate higher predictive power. A sequential (Type 1) analysis was then undertaken: each variable was added in sequence to the model with a likelihood ratio test for model improvement used to assess the value the additional predictor variable. The sequence of the comparison of models was taken from the univariate modeling results (McCullagh and Nelder 1989).

3.0 Results

3.1 Descriptive Analysis

The most fish were released at the 9-, 12-, 15- and 18-m$\cdot$s^{-1} (30, 40, 50 and 60 fps) nozzle velocities (Figure 4) because injuries were rare below 9 m$\cdot$s^{-1} for all species except American shad. A summary of the injury level results compiled from all the species and age groups tested is shown in Figure 5. Major injuries primarily occurred at jet velocities of 12 m$\cdot$s^{-1} or higher and the proportion of major injuries clearly increased with increasing jet velocity. Deaths primarily occurred at the 18-m$\cdot$s^{-1} jet velocity.

Time series plots of the dynamic parameters computed from the digitized fish paths are shown in Figure 6 through Figure 11. The points are connected with straight lines primarily to allow differentiation of each fish. The true value of the parameters between the points calculated is unknown because our sampling rate was limited to one image every 0.004 s. It is clear from the plots that the fish experience abrupt changes in all of the dynamic parameters. Positive and negative values exist for all the variables with the exception of distance, which is why the means were computed from the absolute values of these parameters. Also, the curves for acceleration, impulse, and force are shaped the same. This is because the same mass was used for all age-1 fish and the time step is constant. Subsequently, only velocity, jerk, and force are included in the remaining analysis.

The sequence of images in Figure 12 shows the first 0.024 s of the release of an age-1 spring chinook salmon into the jet at 18 m$\cdot$s^{-1}. The pattern shown in Figure 12 is typical of many of the releases. The fish descends the introduction tube head first and right side up (image 1). Upon initial contact with the jet, the fish begins to turn to its side and one or both of the opercula open (images 2 and 3). The fish then turns completely on its side and the opercula flare completely as it is thrust forward (images 4 and 5). Finally, the fish moves free of the introduction tube and downstream in the turbulent jet flow, which allows the opercula to return to a more normal position (image 6). Because of the mediocre image quality, different parts of the fish could not be tracked precisely.

The sequence of images in Figure 13 shows a bottom view of the first 0.036 s (9 video frames at a 4 milliseconds per frame) of an age-1 fall chinook salmon release at a nozzle velocity of 15 m$\cdot$s^{-1}. The pattern is similar to that of Figure 12. In Figure 13, both opercula catch flow from behind and flare forward upon initial exposure to the water jet. The fish then turns to one side as it continues to exit the introduction tube and enter the jet flow. Maximum deformation of the opercula appears to occur around the sixth frame. Thereafter, the force on the opercula begins decreasing as more of the fish enters the flow and the velocity of the fish increases, which reduces the relative velocity of the jet. Figure 13 also shows that minimal lateral movement occurs during the initial part of the release.
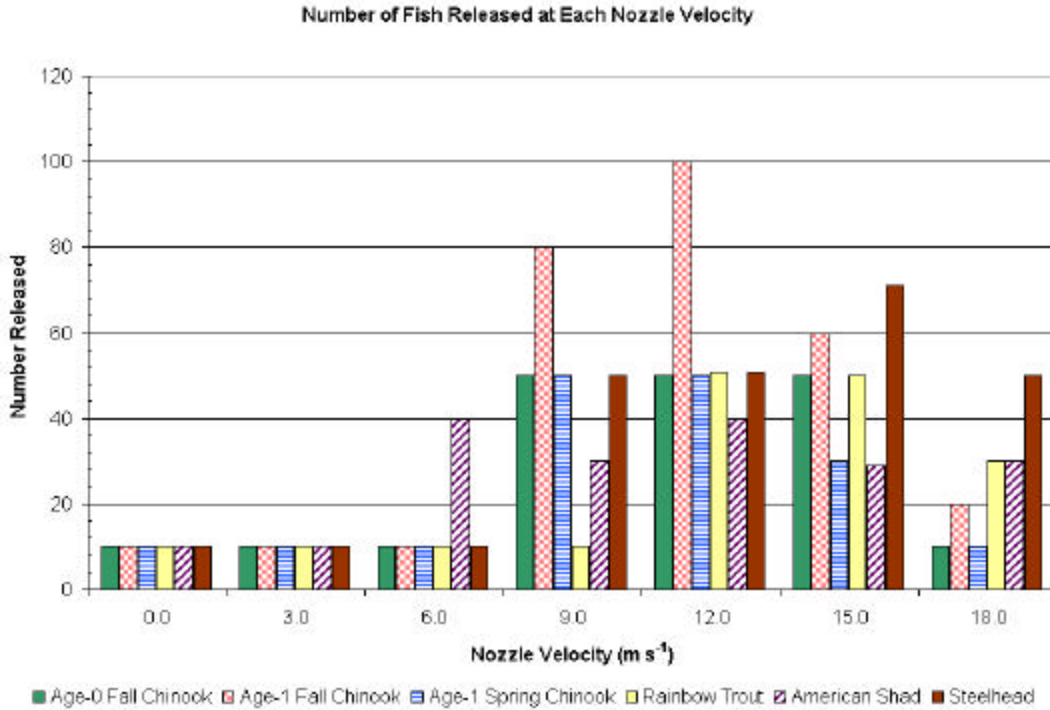
Figure 4. Number of fish released at each nozzle velocity for each species.
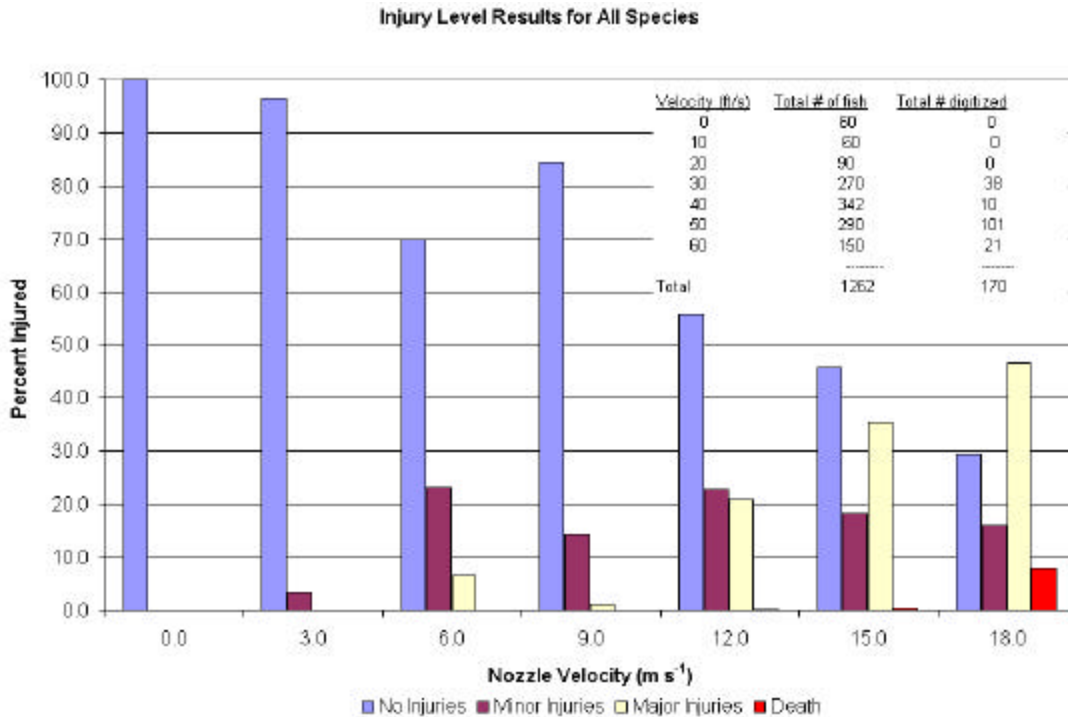
Figure 5. Injury levels for all species. The table in the upper right summarizes the total number of fish released at each velocity.
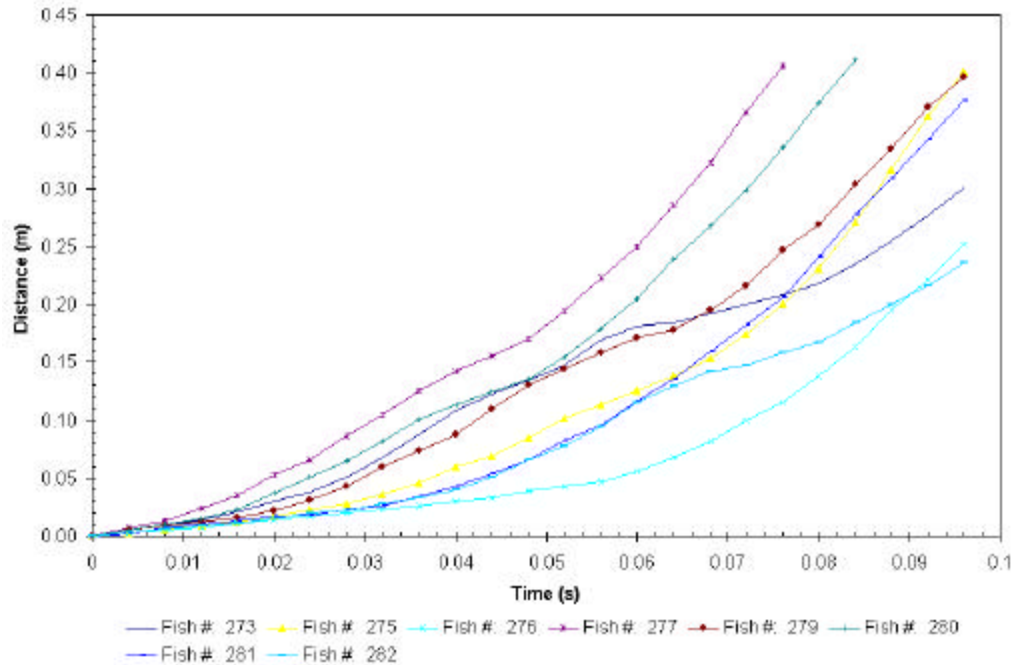
Figure 6. Distance versus time as measured from the digitized paths of a group of age-1 fall chinook salmon at the 15-m·s⁻¹ (50 fps) nozzle velocity. Note: the points are connected with straight lines to facilitate differentiation of each fish. The nature of the transition between points is not necessarily linear.
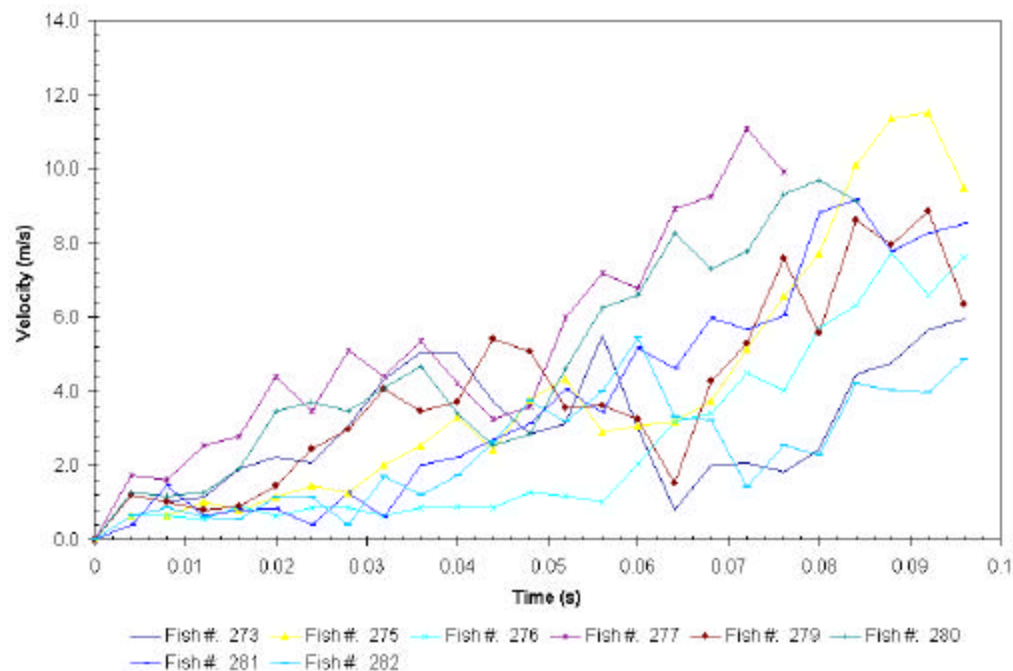
Figure 7. Time series plot of velocity for a group of the age-1 fall chinook salmon released at the 15-m·s⁻¹ nozzle velocity. Note: the points above and in the other time-series plots are connected with straight lines to facilitate differentiation of each fish. The nature of the transition between points is not necessarily linear.
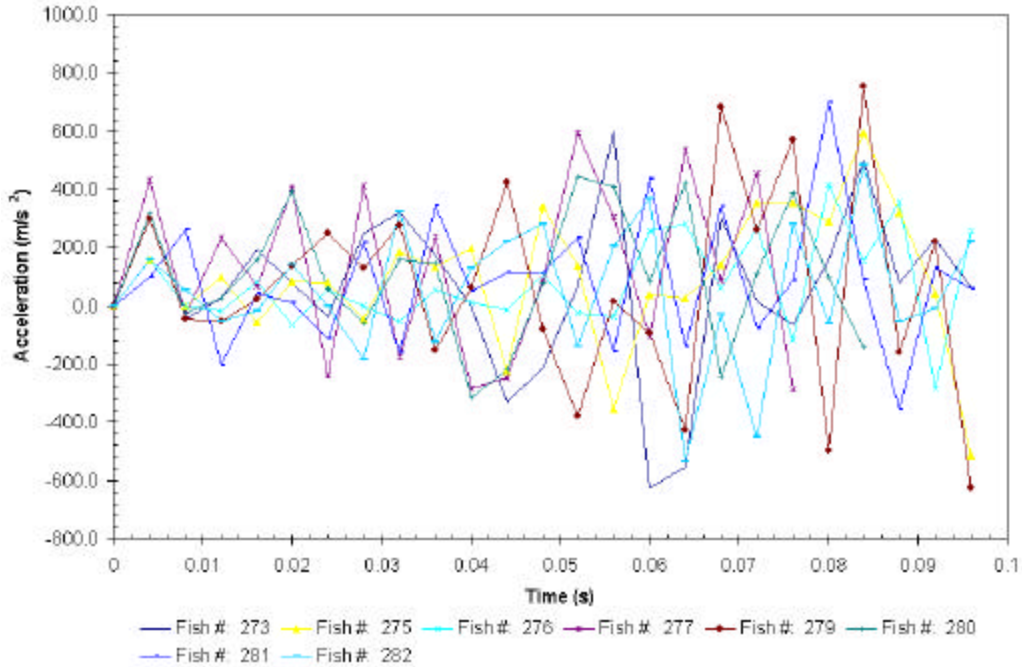
Figure 8. Time series plots of acceleration for a group of the age-1 fall chinook salmon released at the 15-m·s^{-1} nozzle velocity.
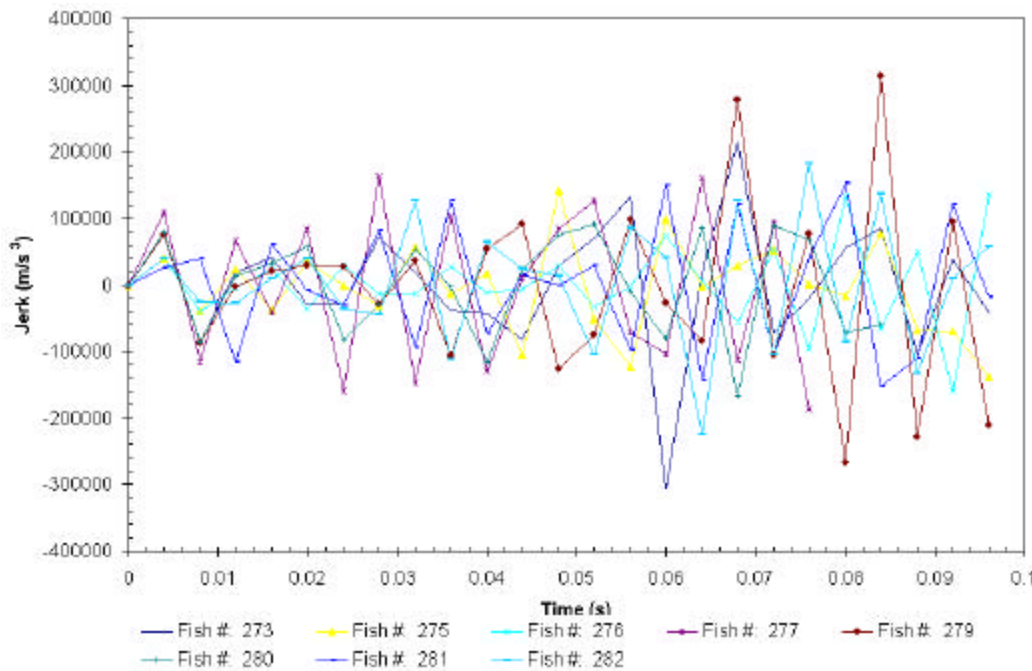
Figure 9. Time series plot of instantaneous jerk (rate of change in acceleration rate) for a group of the age-1 fall chinook salmon released at the 15-m·s^{-1} nozzle velocity.
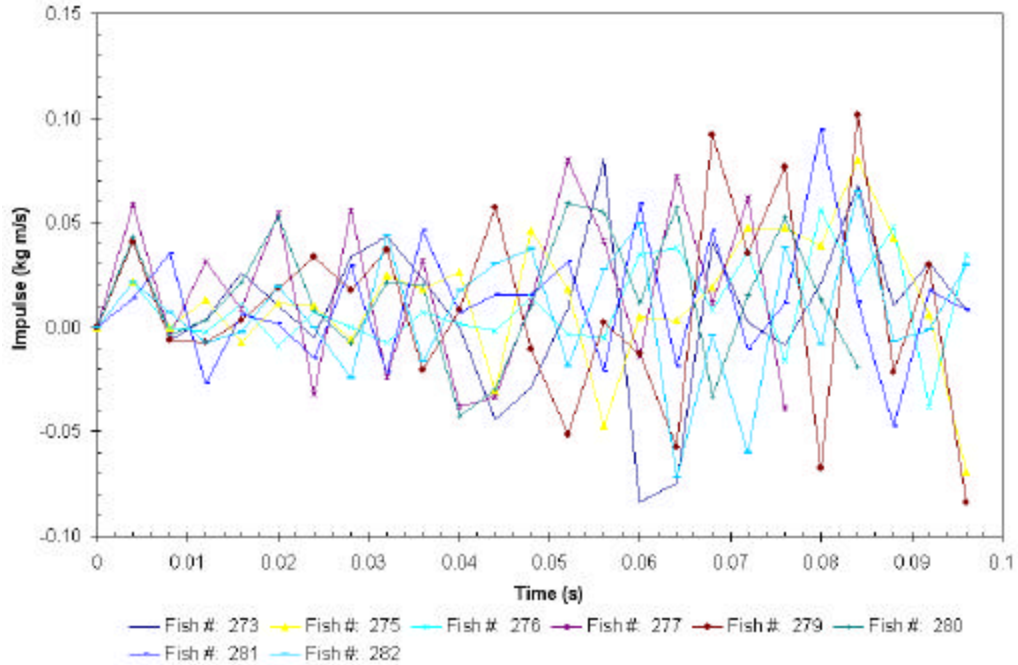
Figure 10. Time series plot of impulse (fish mass*change in velocity) for a group of the age-1 fall chinook salmon released at the 15-m·s^{-1} nozzle velocity.
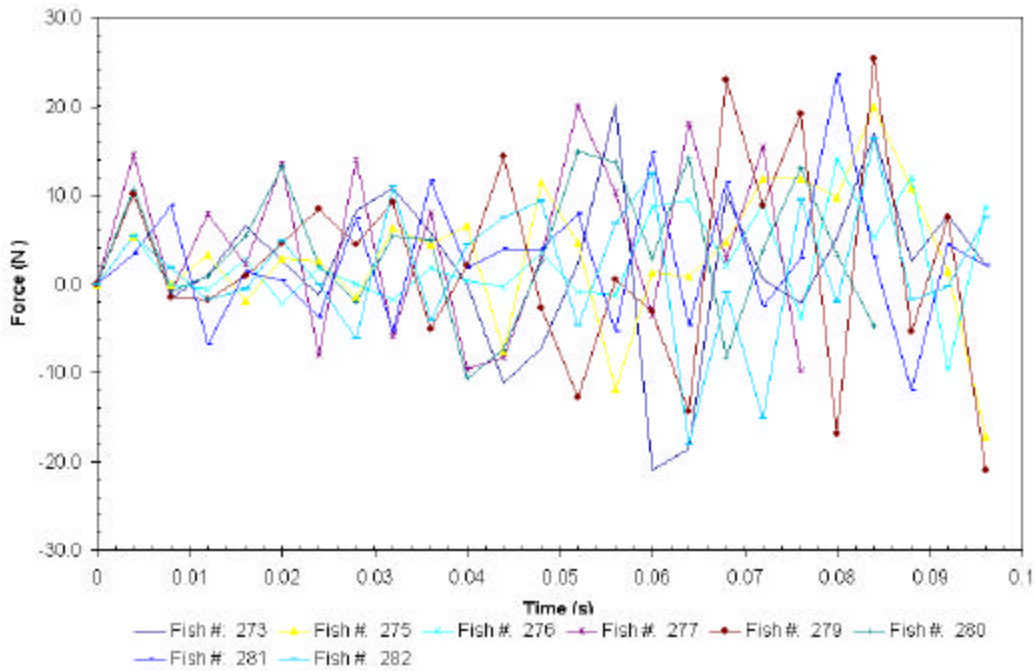
Figure 11. Time series plot of force (mass*acceleration) for a group of the age-1 chinook salmon released at the 15-m·s^{-1} nozzle velocity.
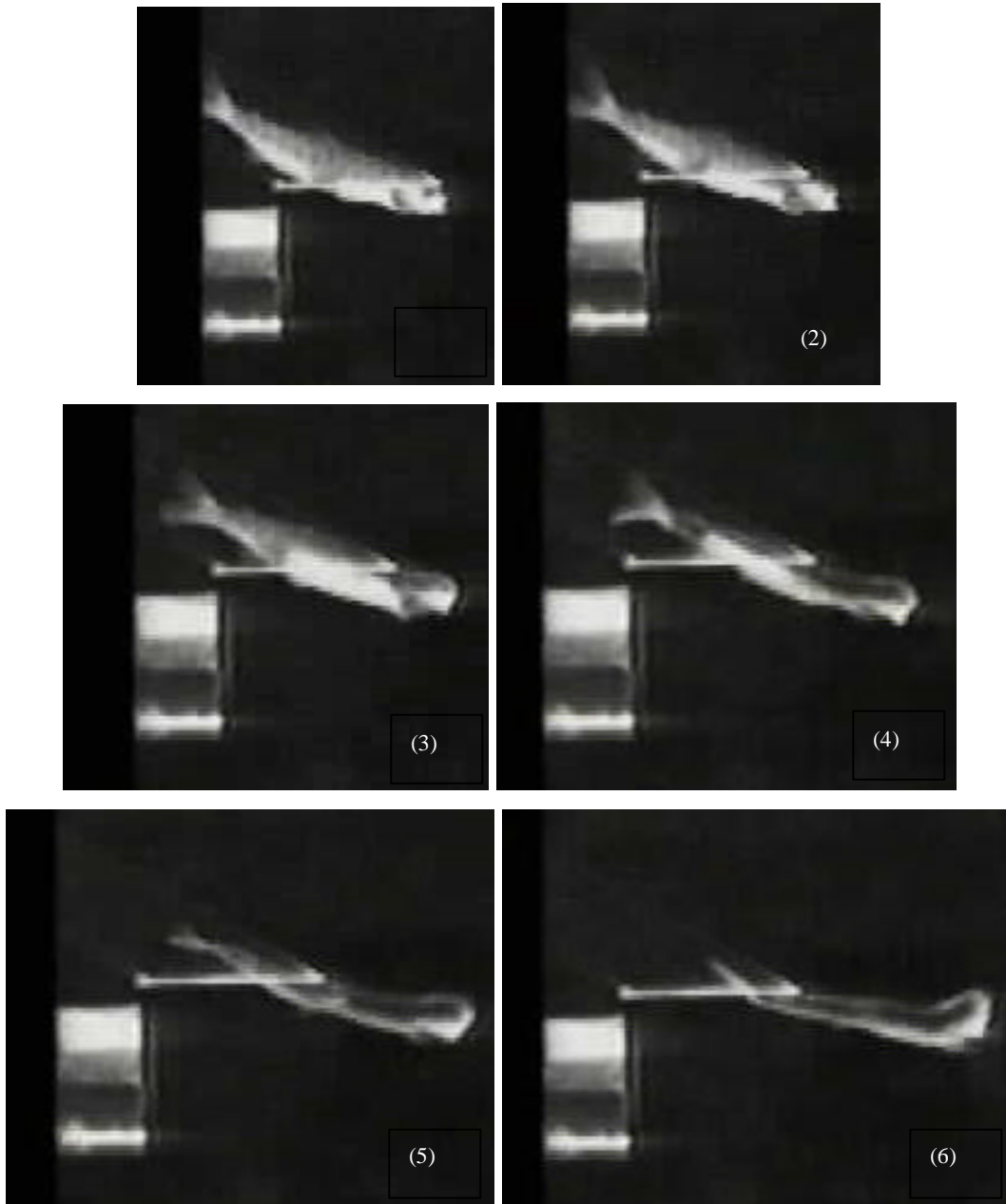
Figure 12. Series of side views showing the initial 0.024 s of an age-1 spring chinook salmon released at an 18-m·s^{-1} jet velocity. Note: the opercula flare wide open in images 2 and 3, and then return to a more normal position by image 6.

The relative proportions of fish in each injury level for the age-0 and age-1 chinook groups are similar (Figure 14 and Figure 15). Major injuries clearly increase with jet velocity above 9 m·s^{-1} for both age classes, and deaths only occur for age-1 fish at 15 and 18 m·s^{-1}. The age-0 fish group has a higher proportion of non-injury and a lower proportion of major injuries at all nozzle speeds.
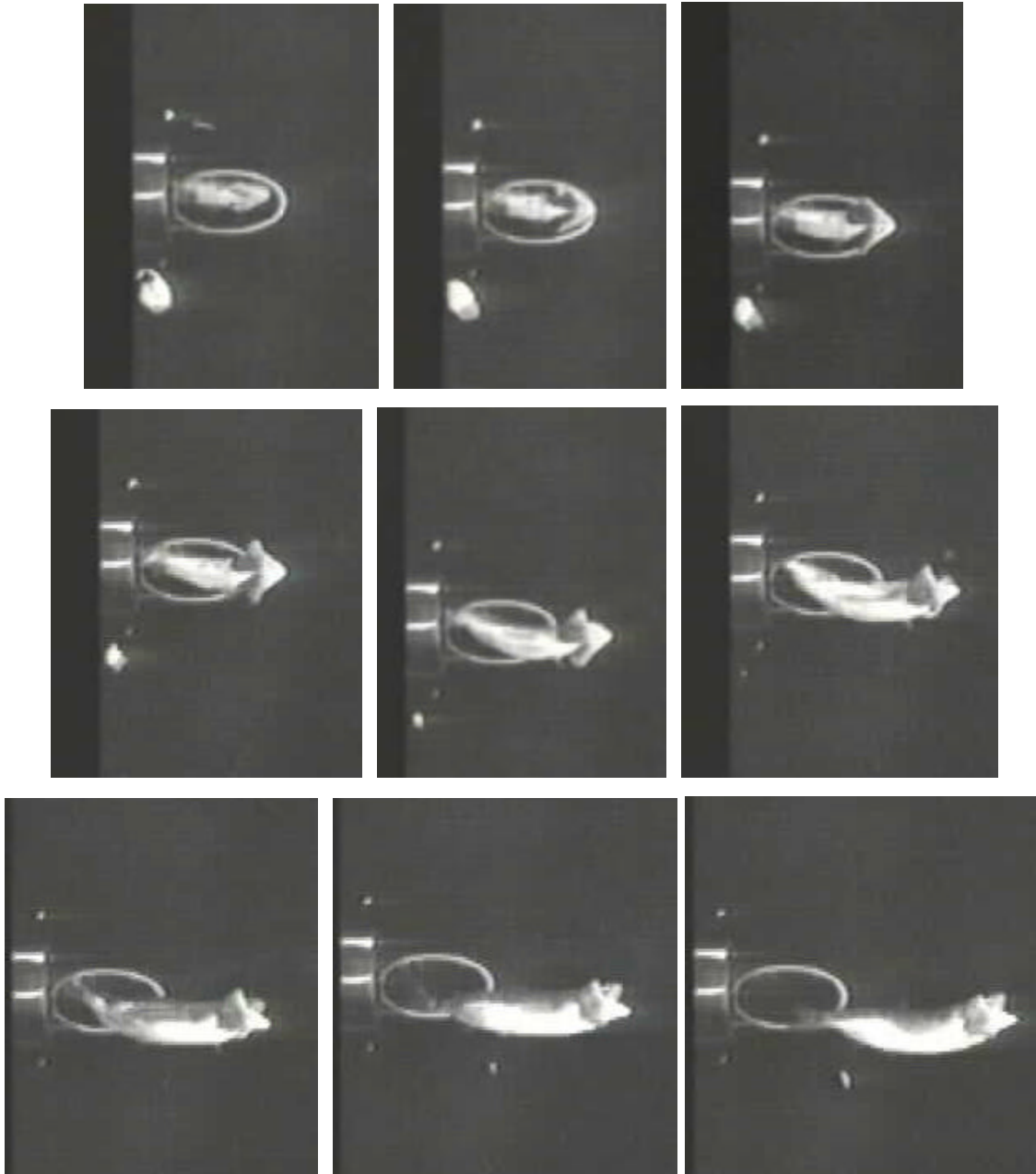
Figure 13. Series of bottom view images showing the initial 0.036 s of an age-1 fall chinook salmon released at a 15-m·s^{-1} jet velocity. Note: both opercula flare upon initial contact with the jet and then the fish turns to one side as it exits the introduction tube.

Additional analyses were focused on the spring and fall chinook salmon groups because these groups combined to form the largest available sample of fish with comparable size and physical characteristics. Relative proportions of injury types for age-0 and age-1 chinook salmon are shown in Figure 16 and Figure 17, respectively. Operculum injuries predominated at the relatively low nozzle velocity of 12 m·s^{-1} for both age groups, where other injuries were rare. Isthmus and operculum injuries were common at 15-m·s^{-1} nozzle velocity for the age-1 fish, while disorientation was common for age-0 fish. At
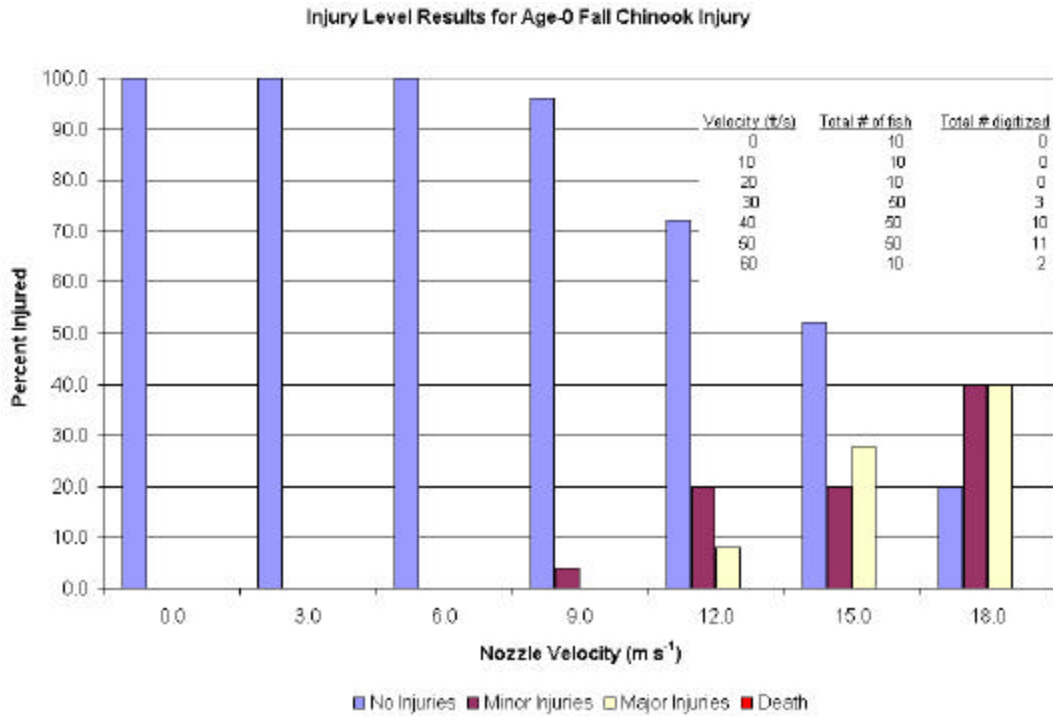
Figure 14. Injury level results of age-0 fall chinook salmon experiments. The table in the upper right summarizes the total number of fish released at each velocity.
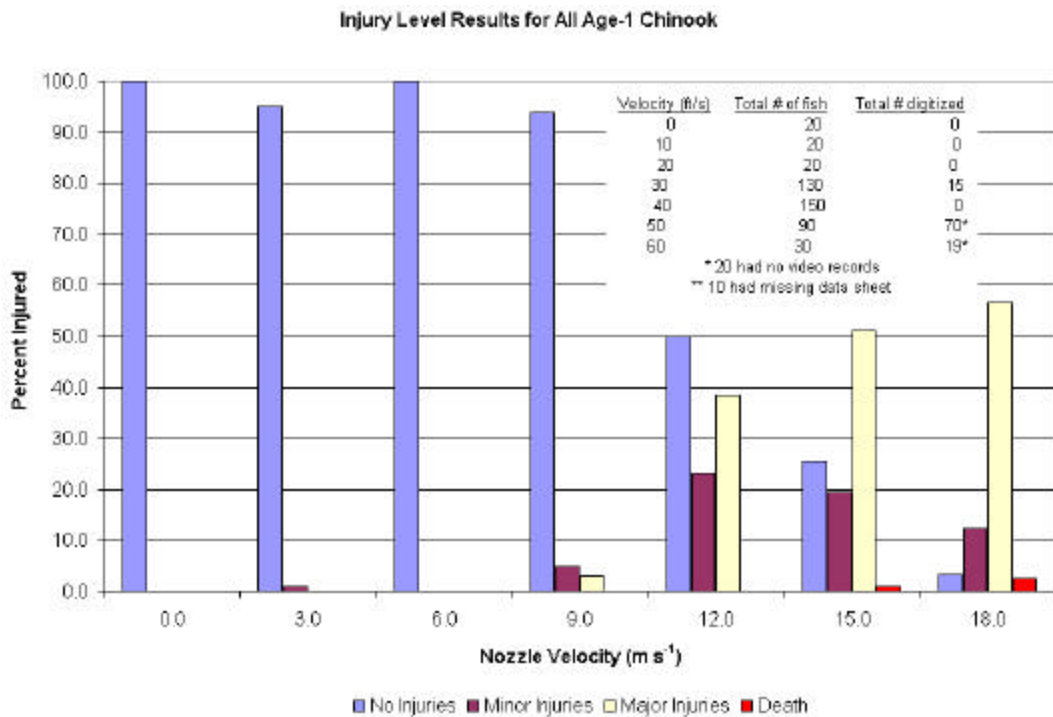
Figure 15. Injury level results of the age-1 spring chinook salmon experiments. The table in the upper right summarizes the total number of fish released at each velocity.

Experimental Results by Injury Type for all Age-0 Chinook
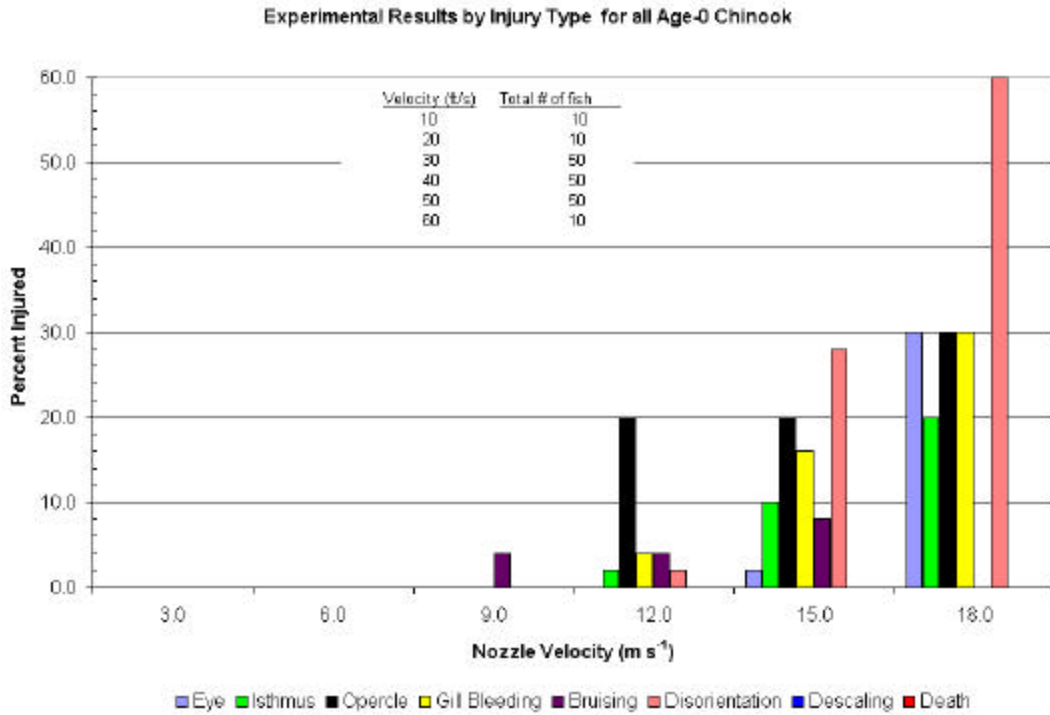
Figure 16. Relative proportions of injury types for all age-0 chinook salmon at each nozzle velocity.

Experimental Results by Injury Type for all Age-1 Chinook
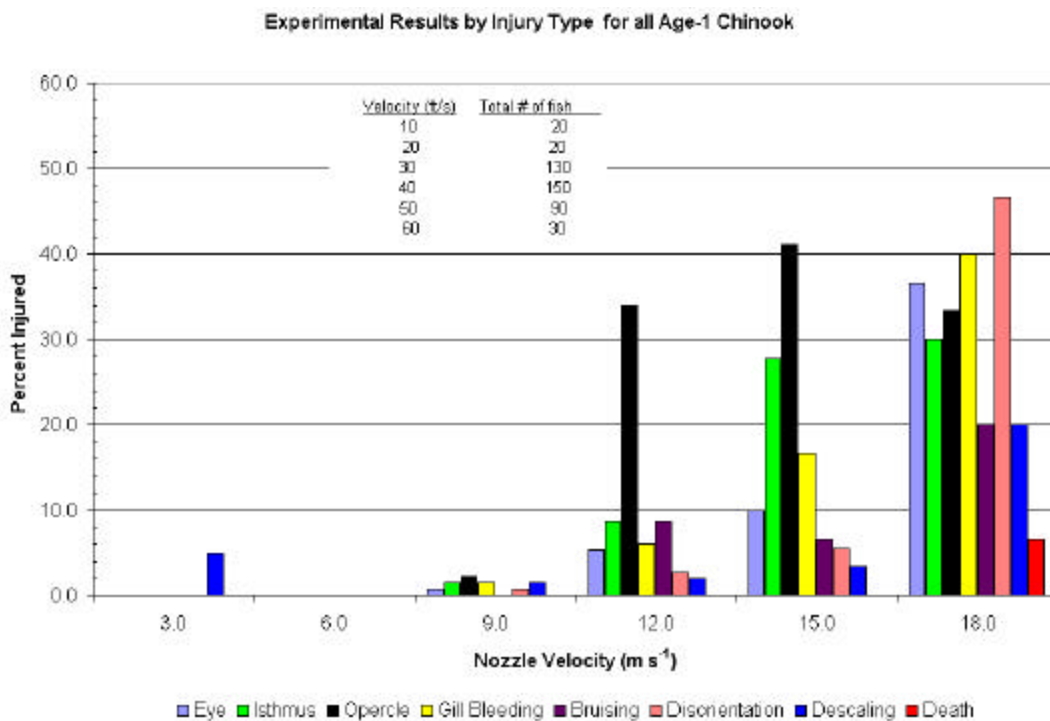
Figure 17. Relative proportions of injury types for all age-1 chinook salmon at each nozzle velocity.

the 18-m·s^{-1} nozzle velocity, multiple injuries became common for both age groups and no particular injury type stood out except for disorientation for age-0 fish. These results suggest the following:

- Operculum injuries predominated at moderate nozzle speeds (12 and 15 m·s^{-1}).
- At the highest nozzle speed, eye, operculum, isthmus, and gill injuries were equally common and disorientation was most common, especially for age-0 fish.
- Bruising and descaling were relatively rare, especially for age-0 fish.
- Age-0 fish had lower proportions of injuries (except disorientation), especially at lower nozzle velocities, which suggests that disorientation may be a more important factor for the younger, smaller fish.

The mean and median dynamic parameter values for each injury level are compared for age-0 and age-1 fish in Figure 18. These values were computed for the first 0.024 s of the fish release (data from each of the first six video frames at 0.004 s between frames). For age-0 fish, the mean and median values of the jerk and force are highest for the major injury group, while the velocity is not significantly different (Figure 18). The high injury group consists of only one fish for the age-0 group, however. Dynamic parameter values are not significantly different between the minor injury and no injury groups. Results for age-1 fish are somewhat more conclusive. The mean and median values of each dynamic parameter are highest for the major injury group, and the differences appear to be significant. The fact that the median is less than the mean in most cases indicates that these distributions are positively skewed, probably as a result of a few disproportionately high parameter values. The significance of these trends will be further examined in the next section.

Figure 18 also provides justification for separating the age-0 and age-1 fish in the descriptive and inferential analysis. Note, the age-0 fish have substantially higher values than age-1 fish for velocity and jerk, and lower values for force. Also, recall that age-0 fish sustained visible physical injuries more rarely and had very few severe injuries and deaths. Therefore, when the age-0 and age-1 groups are combined, the age-0 fish essentially add a large number of individuals with high velocity, acceleration, and jerk values to the low injury group. This causes the lower injury levels to have high values of velocity and acceleration when, in fact, the low injury levels have low values for velocity and acceleration within a given age group. These observations imply that the age-1 fish are more prone to visible physical injuries because they sustain higher levels of force as a result of their increased mass. Alternatively, the age-0 fish may be more prone to disorientation because they experience higher levels of inertial stress from acceleration and jerk as a result of their lesser mass.
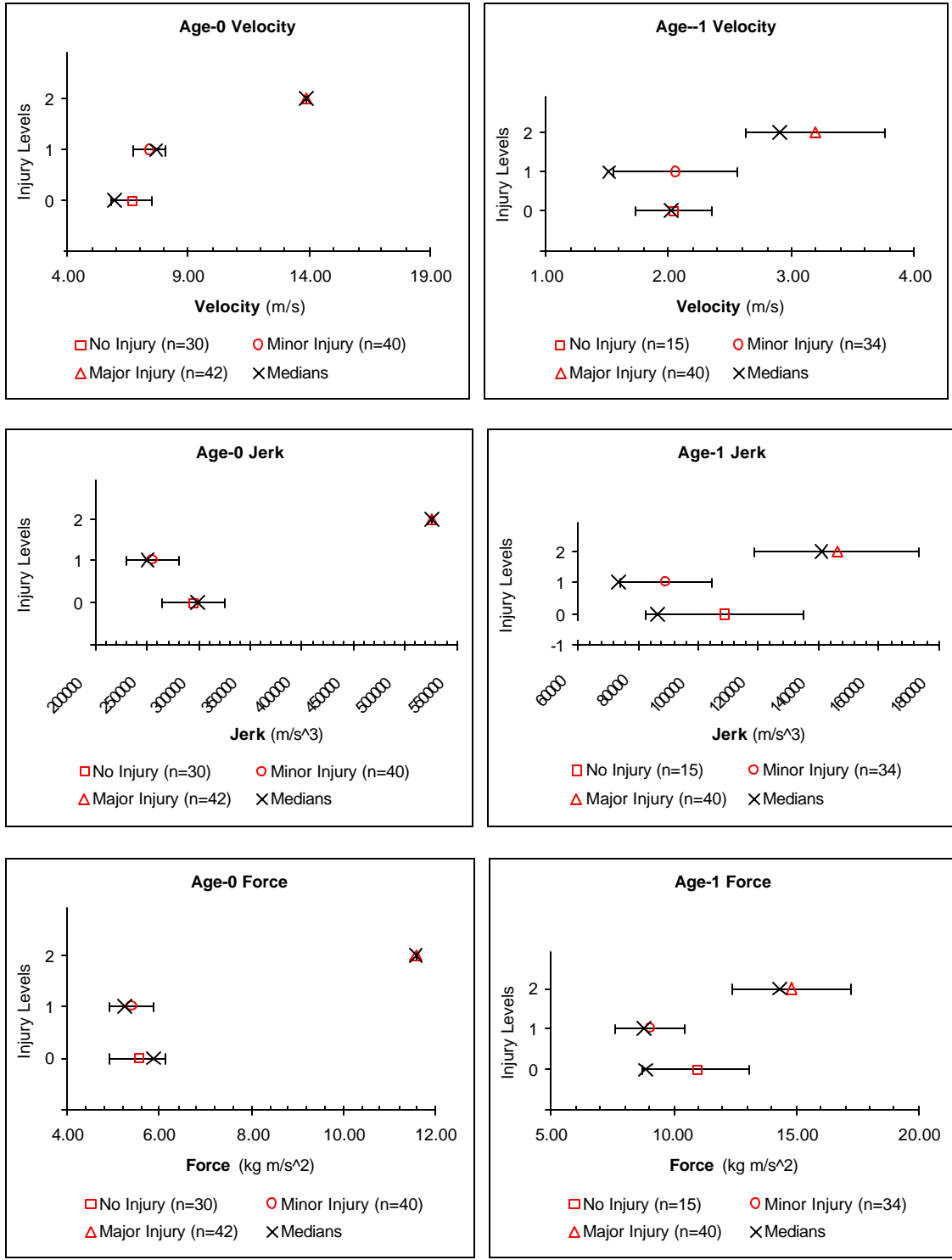
Figure 18. Comparison of means and medians (calculated with initial 0.024 s of data) between each of the three injury le vel groups for all **age-0** and **age-1** chinook salmon. Error bars indicate one standard deviation about the mean. Note: cases where the median is less than the mean indicate that the distributions are positively skewed.

3.2 Inferential Analysis: Multinomial Response Model

The parameter correlations are shown in **Figure 19** for the values computed from the first 0.016 s of the release. Perfectly correlated parameters plot to form a straight line, which indicates that these parameters only differ by a scalar multiplier and, in effect, provide identical information. These correlation plots are equivalent to those computed from 0.024 and 0.10 s data. The plots verify that acceleration correlates directly with impulse and force. Again, acceleration and impulse correlate perfectly because the same average mass was used for all fish, and force and impulse correlate perfectly because dt is a constant 0.004 s ($F= I/dt$). Therefore, the inferential analysis will consider only velocity, jerk, and force.

The univariate modeling results on each of the three time intervals are summarized in Table 2. Also shown in Table 2 are the parameter estimates, standard errors, and t-tests of significance on the estimates. At 0.016 s post-release, each of the three dynamic parameters showed statistical significance in predicting the injury response. The univariate modeling results at 0.024 s post-release were very similar to those at 0.016 s. At 0.10 s following release, the signal-to-noise ratio in the data is sufficiently low to show no significant predictive value in any of the three dynamic predictor variables. Estimates of the coefficients shown in Table 2 are uniformly positive, indicating a positive correlation or larger dynamic parameter values are associated with higher levels of injury.
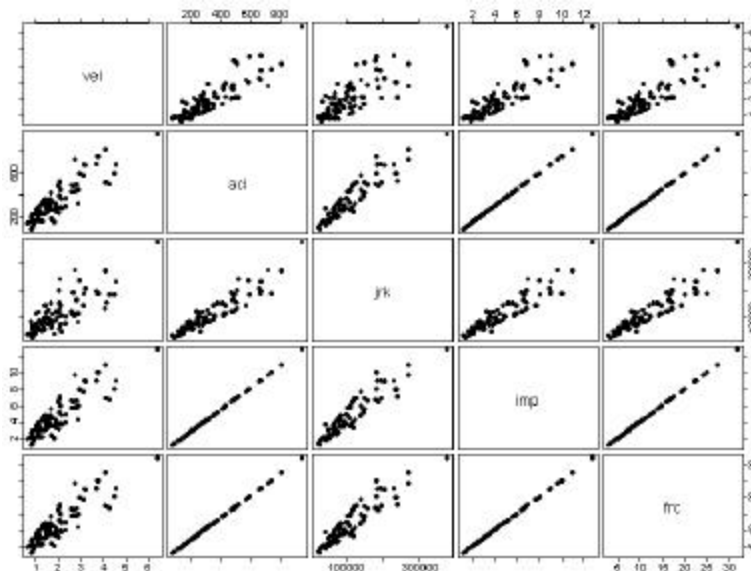
Figure 19. Cross correlation plots derived from the 0.016 s data for each variable examined. Linear plots with no scatter indicate perfect correlations between variables (acceleration, impulse, and force).

Table 2. Univariate modeling summary.

Source	DF	Nobs	ChiSq	P(ChiSq)	Estimate	StdErr	tstat	Prob_t
0.016 Sec								
Force	1	83	15.43	<0.0001	1.785E-01	4.540E-02	3.928	0.079
Velocity	1	83	12.99	0.0003	9.387E-01	2.605E-01	3.604	0.086
Jerk	1	83	12.59	0.0004	1.500E-05	4.175E-06	3.548	0.087
0.024 Sec								
Force	1	83	14.92	0.0001	1.665E-01	4.310E-02	3.862	0.081
Jerk	1	83	12.43	0.0004	1.300E-05	3.736E-06	3.525	0.088
Velocity	1	83	11.13	0.0009	5.942E-01	1.781E-01	3.336	0.093
0.100 Sec								
Force	1	83	1.47	0.2254	1.160E-02	9.600E-03	1.212	0.220
Jerk	1	83	1.44	0.2308	9.297E-07	7.759E-07	1.198	0.221
Velocity	1	83	0.5	0.4797	5.230E-02	7.400E-02	0.707	0.304

Multivariate model selection results for each of the three time intervals are shown in Table 3. A separate model was fit for each time interval. The dynamic parameters were added sequentially to a model taking the injury level as the multinomial response variable. This sequential analysis approach controls for co-linearity among the predictors. From Table 3, force shows the highest predictive power on the level of injury, and adding the other two dynamic parameters of velocity and jerk did not significantly reduce the model deviance. This further demonstrates the high correlation between the three dynamic predictor variables.

Table 3. Multivariate sequential modeling summary.

Source	Res. Dev.	Dev.	NumDF	ChiSq	Prob(ChiSq)
0.016 Sec					
Intercepts	164.5248				
Force	144.7206	19.8042	1	22.07	<0.0001
Velocity	144.7059	0.0147	1	0.02	0.898
Jerk	144.4927	0.2132	1	0.24	0.626
0.024 Sec					
Intercepts	164.5248				
Force	146.1999	18.3249	1	20.24	<0.0001
Jerk	145.9408	0.2591	1	0.29	0.5927
Velocity	145.7699	0.1709	1	0.19	0.6639
0.100 Sec					
Intercepts	164.5248				
Force	162.9785	1.5463	1	1.53	0.2164
Jerk	162.9448	0.0337	1	0.03	0.8552
Velocity	162.9105	0.0343	1	0.03	0.8539

Box plots are shown in Figure 20 for each of the five dynamic parameters (a good reference for interpreting box plots is given by Cleveland (1993), pp. 25-27). The white bar indicates the median, the box indicates the upper and lower quartiles, the brackets indicate a rough 99% confidence interval about the median, and dashes indicate possible outliers or extreme values. The distributions of dynamic parameter values derived from the first 0.016 and 0.024 s of the video records do not appear to be significantly different for any dynamic parameter.

Alternatively, the dynamic parameter values derived from the first 0.1 s of the release are significantly higher than those calculated from the initial 0.016 and 0.024 s of the video records for each of the three parameters, especially for velocity (Figure 20). This is expected as the full path of the fish is captured during the first 0.1 s, including high-velocity tumbling that occurs when the fish is fully entrained into the jet flow. These high, dynamic parameter values seem to confound the statistical results, however, as the videotapes show that the injuries occur during initial contact with the jet, before the fish completely exits the introduction tube. Therefore, conclusions will be drawn from the 0.016 and 0.024 s results.
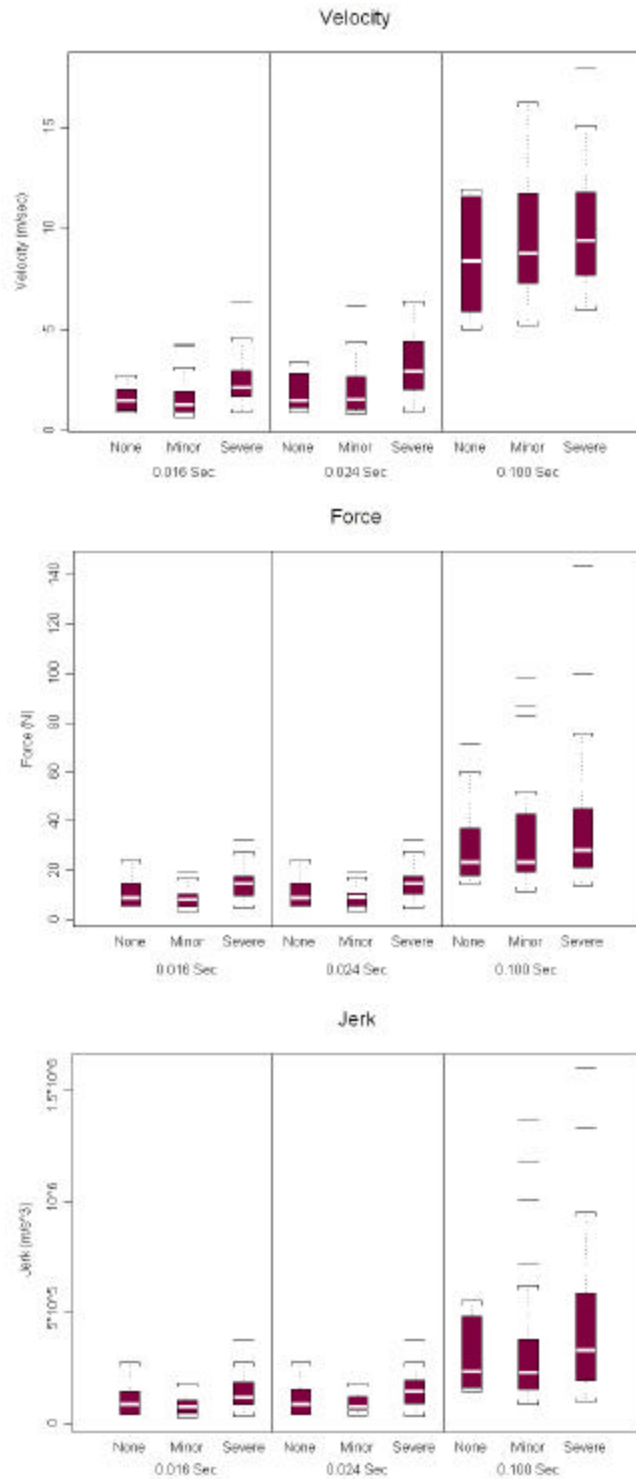
Figure 20. Box plots of dynamic parameters by time interval and injury level. Note: the white bar indicates the median, the box indicates the upper and lower quartiles, the brackets indicate a rough 99% confidence interval about the median, and dashes indicate possible outliers or extreme values.

4.0   Discussion

Looking at the results as a whole, age-0 fish experience higher levels of velocity, acceleration, and jerk; lower levels of force; fewer visible injuries; and greater proportions of disorientation than age-1 fish. These findings suggest that the inertial stresses of higher acceleration and jerk may be the primary cause of the internal injuries and impairments responsible for disorientation in these fish. Alternatively, the forces applied to exposed organs, which are proportional to the mass of the specimen, are more closely associated with visible injuries such as operculum and gill damage.

When similar sized fish are analyzed, the results suggest that of the dynamic parameters estimated from the bulk motion of the fish (velocity, jerk, and force), force is the most predictive of injury. In this study, however, force is essentially equivalent to acceleration because individual fish masses were not used. This strong relative predictive ability of force (and therefore acceleration) makes sense from a biomechanical perspective. The force on the fish is the product of the acceleration and the mass, and is essentially the "push or pull" that the fish experiences upon contacting the jet. In nearly all cases, the force is primarily exerted on the opercula. An additional parameter that could be even more predictive of operculum or isthmus injuries is the differential acceleration between the opercula and the body of the fish, which could not be measured accurately from the videos because of the mediocre image quality.

The video records of the fish releases in this study were originally intended only to provide a means of observing the releases and possibly making crude estimates of the accelerations involved. Therefore, limited resources were devoted to optimizing the quality of the video data, and the video images obtained were subsequently of mediocre quality. The quality of the images was sufficient for the intended purpose of observation. It was, however, insufficient for sophisticated motion analysis and limited the potential to accurately and precisely track the path of the fish and its constituent parts. In future studies incorporating motion analysis, a more advanced video system should be used. Such a system would incorporate clearer viewing windows, improved background lighting control, a strobe light for illumination, and higher resolution digital cameras.

The parameters in this analysis were computed from the initial 0.016 and 0.024 s of the digitized release data because the visible physical injuries were assumed to have occurred during initial contact based on the video records. This assumption is based on the following reasons: (1) during initial contact, the fish is moving very slowly and thus the velocity differential is greatest, and (2) during initial contact, the smallest contact area exists, with either the eye or the operculum usually making contact first. The maximum accelerations generally occur once the full body of the fish is in the jet flow and the contact area is at a maximum. Using only the first instance of the introduction also provides the added benefit of reducing the error associated with digitizing the path of the eye and not the centroid.

This type of video analysis could be improved in a number of ways to better characterize the injury process and quantify the dynamic parameters involved. Primarily, the motion of the fish should be tracked in sufficient detail to resolve the relative motion of different body parts. In addition, using a balanced orthogonal study design would make the analysis more robust. A balanced orthogonal study design would have equal representation for all factors and factor levels (i.e., equal numbers of age-0 and age-1 fish allocated equally to each nozzle speed). Recording the mass of each individual fish would also improve the predictive power for the dynamic parameters computed using mass (impulse and force) and would allow differentiation between force and acceleration. Using the actual mass of each test fish would also help to blend the distinction between the age-0 and age-1 groups, perhaps making it possible to combine all the fish into a single continuous population. Additionally, these individual masses should be included in the data set as a predictor variable for injury because low-mass fish are less prone to visible injuries and more prone to disorientation. Impulse could probably be dropped from future studies because it will be essentially equivalent to force as long as the time step, generally some multiple of the camera frame rate, is constant.

Additional variables that could be investigated in a more detailed analysis include the radius of curvature, the angular acceleration, and the angular jerk of the fish. The radius of curvature indicates the degree of bending, which may cause bruising along the sides of the fish. Angular acceleration and angular jerk are analogous to linear acceleration and jerk, although they apply to the rotational motion of the fish, which may cause disorientation. In addition, the component vectors ($v_x, v_y, a_x, a_y...$) for each parameter could be included into the analysis in addition to the magnitude, which was analyzed in this study. Including the vector components would reveal the effects of forces in each direction and it would preserve the details of the true path of the fish.

5.0 Conclusions

Visible external injuries in fish released into a characterized submerged water jet generally occurred during the initial contact with the jet and not during the tumbling that occurred after the fish fully entered the turbulent flow. The inertial stresses of tumbling (linear and angular acceleration and jerk), however, may cause temporary or even permanent injuries to the vestibular and neurological systems. Such injuries can then result in behavioral impairments, such as disorientation and loss of equilibrium, that are life threatening in the "natural" environment.

Operculum injuries predominated at moderate nozzle speeds (12 and 15 $m \cdot s^{-1}$). At the highest nozzle speed, eye, operculum, isthmus, and gill injuries were equally common, and disorientation was most common. Bruising and descaling were relatively rare, especially for age-0 fish.

Age-0 fish were less susceptible than the larger age-1 fish to all visible injury types, especially at lower nozzle speeds. This is presumably because age-0 fish have less mass and inertia, and therefore sustain smaller forces on exposed organs during acceleration. Alternatively, age-0 fish were substantially more susceptible to life-threatening behavioral impairments such as disorientation. This again may relate to the smaller mass of the age-0 fish. The less massive age-0 fish sustain larger accelerations and jerks, which are probably important sources of the internal injuries to the vestibular and neurological systems that cause disorientation.

The results of this analysis provide evidence to suggest that all the dynamic parameters computed from the bulk motion of the fish (velocity, jerk, and force) are positively correlated with injury level. Multinomial response model results further suggest that the force parameter is most predictive of injury.

6.0   References

Cleveland, WS. 1993. *Visualizing Data.* Hobart Press, Summit, NJ.

McCullagh, P and JA Nelder. 1989. *Generalized Linear Models*. Chapman and Hall, New York City.

Neitzel, DA, MC Richmond, DD Dauble, RP Mueller, RA Moursund, CS Abernethy, GR Guensch, and GF Cada. 2000. *Laboratory Studies on the Effects of Shear on Fish: Final Report*. Prepared for the U.S. Department of Energy, Idaho Operations Office, Idaho Falls, ID, by the Pacific Northwest National Laboratory, Richland, WA.

Zar, JH. 1999. *Biostatistics*, Fourth Edition, eds. T Ryu and SL Snavely, pp. 76-78. Prentice Hall Inc., Upper Saddle River, NJ.

Appendix

Excerpt from data compilation table.

Strain Rate (cm/s/cm)	Velocity (m/s)	Fish Type	Fish ID	Injury Level	Eye	Isthmus	Operculum	Gill Bleeding	Bruising	Disorientation	Descaling	Velocity	Acceleration	Jerk	Impulse	Force
688	12.5	FC 0	067	1			L					553.94	95052.00	23763000.14	2.09	5.23
688	12.5	FC 0	069	0								767.04	70202.36	32365166.44	1.54	3.86
688	12.5	FC 0	070	1				R				637.70	111252.84	40414170.36	2.45	6.12
688	12.5	FC 0	071	0								768.40	93173.33	23990732.23	2.05	5.12
688	12.5	FC 0	072	0								597.59	71492.71	28979410.58	1.78	4.44
688	12.5	FC 0	073	0								557.41	90307.33	35926580.43	1.99	4.97
688	12.5	FC 0	076	0								1042.68	119877.19	38205471.60	1.86	4.64
688	12.5	FC 0	077	0								872.59	140545.89	55724861.60	3.09	7.73
688	12.5	FC 0	078	0								668.36	107080.74	26770185.32	2.36	5.89
688	12.5	FC 0	079	0								741.79	81006.68	33393956.64	1.78	4.46
852	15.2	FC 0	035	0						1		1189.60	118707.26	43178880.04	2.61	6.53
852	15.2	FC 0	037	1					L			1174.27	135963.38	27901512.03	2.99	5.09
852	15.2	FC 0	039	0								877.82	139437.50	34859375.00	3.07	7.67
852	15.2	FC 0	040	1			L					1287.92	107873.99	34446724.48	2.37	5.93
852	15.2	FC 0	082	1			L					836.29	81006.68	24967897.52	1.78	4.46
852	15.2	FC 0	083	0						1		1194.73	142280.99	41588095.36	3.13	7.83
852	15.2	FC 0	084	1			R					1372.93	112587.15	33585237.85	2.48	6.19
852	15.2	FC 0	085	0								1067.93	128380.54	49329906.22	2.82	6.58
852	15.2	FC 0	086	1			R					716.34	85819.92	39774785.00	1.89	4.72
852	15.2	FC 0	087	0								1005.44	117441.36	27248047.73	2.58	6.46
852	15.2	FC 0	088	0						1		716.73	117415.37	38823322.46	2.58	6.46
1008	18.3	FC 0	012	0								1139.58	120937.82	42751744.48	2.66	6.65
1008	18.3	FC 0	019	2		1						1510.99	210752.53	52573670.59	4.64	11.59
852	15.2	FC 1	081	0							1	500.24	110000.32	54343216.81	2.42	6.05
852	15.2	FC 1	083	1	R		R					1423.66	246501.75	100194608.1	5.42	13.56
852	15.2	FC 1	085	2	R		R			1		1343.94	186596.20	73406591.56	4.11	10.26
852	15.2	FC 1	087	2			R					1176.12	144865.42	64995460.14	3.19	7.97
852	15.2	FC 1	089	0								1167.48	210988.35	48200721.66	4.64	11.60
852	15.2	SC	042	1			LR					1465.60	137117.78	58717510.26	3.02	7.54